Inorganic Chemistry

Article

pubs.acs.org/IC

Tunability of Band Gaps in Metal–Organic Frameworks

Chi-Kai Lin,[†,‡] Dan Zhao,[†] Wen-Yang Gao,[§] Zhenzhen Yang,[‡] Jingyun Ye,[∥] Tao Xu,[‡] Qingfeng Ge,[∥] Shengqian Ma,*[,†,§] and Di-Jia Liu*[,†]

[†]Chemical Sciences and Engineering Division, Argonne National Laboratory, 9700 South Cass Avenue, Argonne, Illinois 60439, United States

[‡]Department of Chemistry and Biochemistry, Northern Illinois University, DeKalb, Illinois 60115, United States

[§]Department of Chemistry, University of South Florida, 4202 East Fowler Avenue, Tampa, Florida 33620, United States

[∥]Department of Chemistry and Biochemistry, Southern Illinois University, Carbondale, Illinois 62901, United States

Supporting Information

ABSTRACT: The tunability of the band gaps in Zn-based metal–organic frameworks (MOFs) has been experimentally demonstrated via two different approaches: changing the cluster size of the secondary building unit (SBU) or alternating the conjugation of the organic linker.

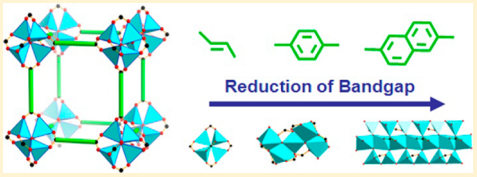

INTRODUCTION

Metal–organic frameworks (MOFs)[1,2] have attracted a great deal of attention from both academia and industry due to their potential in various applications. Their high specific surface areas and well-defined porosities present them unique advantages as new types of adsorbents for gas storage[3,4] and separation.[5,6] The tunable chemical and physical properties through manipulation of composition have led to increasing interest in exploiting MOFs' applications in catalysis,[7−9] as sensors,[10−12] for drug delivery,[13−15] etc.

MOFs are composed of organic ligands that link the metal ions or metal oxide clusters orderly to each other to form the framework. These ionic or oxide centers are also known as secondary building units (SBUs).[16−20] As such, the entire MOF structure is composed of ligand–SBU interfaces. The electronic properties of MOFs, therefore, could be strongly influenced by the interfacial energy level realignments at these interfaces. This unique feature offers the feasibility of chemically tuning the bulk electronic properties of the MOF by exchanging the linkers and/or SBUs. Such versatility paves the way for MOFs to be explored as a new type of semiconductor. For example, when MOFs were prepared with the conjugated carboxylate organic ligands and d^{10} metal clusters (e.g., Zn^{2+}, Cd^{2+}), they were found to exhibit semiconductor behavior.[21−25] When a MOF is treated as a light-sensitive semiconductor, the SBU of the metal oxide cluster can be considered as a discrete quantum dot analogue, which is stabilized and interconnected by the conjugated organic linkers acting as the photon antenna. Although theoretical calculations have found that the band gaps of MOFs are dominated by the energy differences between the highest occupied orbitals (HOMOs) and the lowest unoccupied molecular orbitals (LUMOs) of the organic linkers and can be controlled between 1.0 and 5.5 eV via ligand functionalization,[26] their actual values as the function of ligand conjugation require experimental measurement.[27] In addition, it is well known that the band gaps of quantum dots can be altered by adjusting their sizes.[28] Therefore, it is also possible to tune the band gaps of MOF-based semiconductors by changing the dimensions of the metal cluster SBUs. The cross references of the band-gap changes as a function of ligand conjugation and metal cluster size could improve our understanding on the interaction between these MOF building blocks. In this contribution, we demonstrate for the first time that increasing the sizes of Zn-based SBU clusters leads to a red shift in band gaps of MOFs. We also investigated the influence the conjugation of the carboxlate linkers has on MOFs' band gaps. The results are compared with the calculated band gaps using density functional theory (DFT) methods.

EXPERIMENTAL SECTION

Preparation of MOF-5.[29] Zinc nitrate hexahydrate (360 mg) and 1,4-benzenedicarboxylic acid (66 mg) were dissolved in 10 mL of diethylformamide (DEF) in a 20 mL glass vial with a Teflon-lined lid. The glass vial was placed in an oven and heated to 85 °C (increasing rate 1.0 °C/min) for 12 h and then cooled to room temperature (decreasing rate 0.2 °C/min). Solvent was decanted very quickly, and the remaining solid was first washed three times with 10 mL of anhydrous DMF and then six times with 50 mL of anhydrous $CHCl_3$, each time letting the solid soak in $CHCl_3$ for 8 h. After the final $CHCl_3$ wash, the solvent was decanted quickly and the included $CHCl_3$ was removed under vacuum (10^{-3} Torr, 4 h) to give colorless cube-shaped crystals.

Preparation of IRMOF-8.[30] IRMOF-8 was prepared in a similar procedure to MOF-5. Instead of 1,4-benzenedicarboxylic acid, 2,6-naphthalene dicarboxylate acid (90 mg) was used for the reaction.

Preparation of MOF-FMA:[31] Zinc nitrate hexahydrate (150 mg) and fumarate acid (FMA, 60 mg) were dissolved in 10 mL of DEF in a 20 mL glass vial with a Teflon-lined lid. The glass vial was placed in an oven and heated to 100 °C (increasing rate 1.0 °C/min) for 24 h and

Received: June 4, 2012
Published: July 27, 2012

dx.doi.org/10.1021/ic301189m | Inorg. Chem. 2012, 51, 9039−9044

then cooled to room temperature (decreasing rate 0.2 °C/min). Solvent was decanted very quickly, and the remaining solid was first washed three times with 10 mL of anhydrous DMF and then six times with 50 mL of anhydrous $CHCl_3$, each time letting the solid soak in $CHCl_3$ for 8 h. After the final $CHCl_3$ wash, the solvent was decanted quickly and the included $CHCl_3$ was removed under vacuum (10^{-3} Torr, 4 h) to give yellow-brown cube-shaped crystals.

Preparation of IRMOF-9.[30] 4,4′-Biphenyldicarboxylic acid (BPDC, 30 mg) and zinc nitrate hexahydrate (180 mg) were stirred for 15 min in 10 mL of *N*,*N*-dimethylformamide (DMF) in a 20 mL glass vial. The vial was tightly capped and heated at a rate of 1 °C/min to 100 °C and remained at 100 °C for 18 h. The sample was cooled to 25 °C at a cooling rate of 0.2 °C/min. After decanting the hot mother liquor and rinsing with DMF, the product was immersed in chloroform (Fisher) for 3 days, during which the activation solvent was decanted and freshly replenished three times. Solvent was removed under vacuum at room temperature, yielding the porous material.

Preparation of Zn_5–BPDC.[32] Zinc nitrate hexahydrate (6 mg), BPDC (12 mg), and DMF (3.0 mL) were placed in a 5 mL vial to form a solution under stirring. After being stirred in air for 4 h, the vial was set in a 20 mL glass vial containing an EtOH solution (2.0 mL) of diisopropylanmine (DIPA, 4 drops) and then sealed and left undisturbed for 3 days at 60 °C (1 °C increase, 0.1 °C decrease). After decanting the mother liquor, the product was soaked in CH_2Cl_2 for 24 h and then calcinated at 60 °C for 1 h to remove the included solvent molecules.

Preparation of CPO-7.[33] A mixture of zinc nitrate hexahydrate (150 mg), BPDC (108 mg), pyridine (6 mL), and water (7 mL) was heated to 180 °C in a Teflon-lined steel autoclave for 24 h. Product was washed with water and dried in air at 60 °C.

Optical Band-Gap Measurements. Diffuse reflectance spectroscopy was used to estimate the optical band gaps of MOFs and corresponding ligands. After nonvolatile solvents were replaced by volatile solvents, followed by drying in a glovebox, thin films of samples were prepared in the same glovebox by compressing powders under a pressure of 20 psi for 2 min with the thickness of the films in the range of several micrometers. The films were subsequently sandwiched between two quartz plates and edge sealed by paraffin tape. Spectra were obtained using a UV–vis spectrometer (USB2000, Ocean Optics, Inc.). The light sources of the apparatus were a deuterium lamp and a halogen lamp (DH-2000, Mikropack).

Diffuse reflectance spectra were translated into the absorption spectra by the Kubelka–Munk method.[34] The energy gap (E_g) can be derived from the dependence of $\alpha h\upsilon^2$ (α = absorption coefficient) on the photon energy $h\upsilon$. Extrapolating the tangential line from the high photon energy intersected $\alpha h\upsilon^2$ at $h\upsilon = E_g$. The intensities of $(\alpha h\upsilon)^2$ were normalized according to their 1/4 maximum values to be expressed in one graph.

We also measured the optical absorption of the isolated ligands used for MOF synthesis in this study. The free ligands in their acid form were dissolved in dimethyl sulfoxide (DMSO) in several highly diluted concentrations to mitigate potential π–π stacking between the ligands. We found no detectable shift in the absorption edge between 0.2 and 2 mM in concentration. Thus, we collected the data at 2 mM for better signal-to-noise ratio.

Photoluminescence (PL) Studies. Photoluminescence spectra of all samples were collected on a Hitachi F2500 fluorometer. The wet slurries (wetted by DMSO) of MOF and ZnO powder samples were smeared onto a quartz slide. The quartz slide was placed vertically along the diagonal direction in a quartz cuvette, allowing the incident excitation beam to be 45° from the normal of the quartz slide. The PL detection axial is at a right angle to the incident excitation beam. All samples were measured at 337 nm (excitation wavelength), and PL spectra were collected between 360 and 600 nm with a Newport 337 nm long-pass interference filter on the detector. A 10 nm excitation slit width was used for all samples. Different emission slit widths (2.5, 5, 10 nm) were used for different samples depending on their emitting intensity. Generally, a larger slit width was used for weakly emitting samples to get more signals.

DFT Calculations. Periodic density functional theory calculations were mainly carried out using the Vienna ab initio simulation package (VASP).[35,36] The projector augmented wave method was employed to describe the interactions between ion and electrons.[37,38] The exchange and correlation energy was evaluated using the Perdew–Burke–Ernzehof (PBE) form of the generalized gradient approximation (GGA) functional.[39] The cutoff energy for the plane wave basis set was set to 400 eV. Brillouin zone integration was sampled at the gamma point due to the large size of the unit cell. Atomic structures were optimized using the conjugated gradient algorithm and/or the quasi-Newton scheme until the forces on all atoms were less than 0.03 eV/Å. The band gap was taken as the difference between the highest occupied (HO) eigen state and the lowest unoccupied (LU) eigen state. This method of determining the band gap is well justified as the energy dispersion is small within the first Brillouin zone.

The unit cells of MOF-FMA, IRMOF-9, and IRMOF-8 have 280, 332, and 568 atoms, respectively, and are too big to handle routinely by plane-wave-based programs such as the VASP code. As such, the band gaps of MOF-FMA and IRMOF-8 were calculated using the linear-scaling Siesta code,[40] with the LDA pseudopotentials and a double-ζ basis set. For validation, we calculated the band gap of MOF-5 with both codes and obtained a value of 3.52 eV from VASP and 3.55 eV from Siesta. We kept the parameters in the calculations of MOF-FMA, IRMOF-9, and IRMOF-8 similar to that of MOF-5 and, therefore, believed that the results from the two program packages were comparable.

RESULTS AND DISCUSSION

To evaluate the effect of SBU cluster size on the band gap, we selected three Zn-based MOFs: IRMOF-9,[30] Zn_5–BPDC,[32] and CPO-7,[33] all of which were constructed from the ligand biphenyl dicarboxylate (BPDC) for the "proof-of-concept" studies. IRMOF-9 has a roughly cubic structure of double interpenetration (Figure S1, Supporting Information), with BPDC ligands linking 6-connected Zn_4O_{13} SBUs (Figure 1a). Zn_5–BPDC consists of a 3D framework with an expanded diamondoid topology constructed from double 4-connected Zn_5O_{22} SBUs (Figure 1b) linked by rigid BPDC ligands (Figure S2, Supporting Information). CPO-7 crystallizes in the monoclinic space group *C*2/*c*; the inorganic zinc hydroxide layers serving as infinite SBUs (Figure 1c) contain four-, five-,

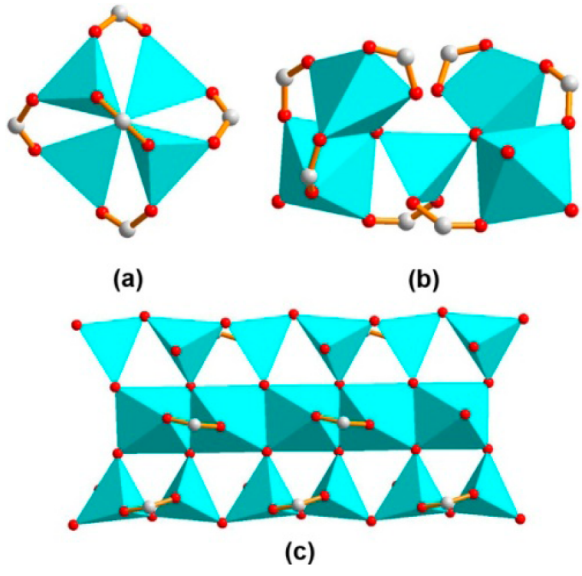

Figure 1. Different size of SBU clusters: (a) IRMOF-9, (b) Zn_5–BPDC, and (c) CPO-7. Color scheme: turquoise polyhedra, Zn; red sphere, O; white sphere, C.

dx.doi.org/10.1021/ic301189m | *Inorg. Chem.* 2012, 51, 9039–9044

and six-coordinated zinc atoms and are pillared by BPDC ligands, leading to a stairway-like configuration along the [001] direction (Figure S3, Supporting Information). The sizes of Zn-based SBU clusters follow the order CPO-7 > Zn_5–BPDC > IRMOF-9. Assuming a similar contribution from the BPDC ligand, we may therefore expect that the changes in the band gap of MOFs are mainly attributed by the SBU cluster size.

IRMOF-9, Zn_5–BPDC, and CPO-7 were prepared and activated according to the procedures in the literature.[30,32,33] Samples were identified by powder X-ray diffraction patterns (Figure S4, Supporting Information), and the same batch of samples was stored in mother liquid until band-gap measurement.

The optical band gaps of the MOFs and their corresponding ligands were measured by collecting the diffuse reflectance spectra at ambient temperature on a UV–vis spectrometer. As shown in Figure 2, IRMOF-9 has a band gap of 3.42 eV while

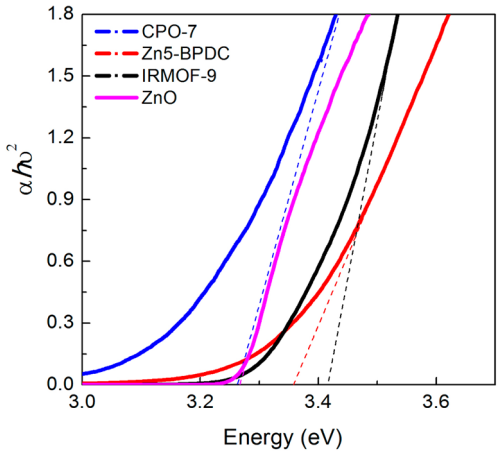

Figure 2. Optical band-gap energy of IRMOF-9, Zn_5–BPDC, CPO-7, and ZnO. Solid lines of blue, pink, red, and black are relation of $(\alpha h\upsilon)^2$ versus the photon energy $(h\upsilon)$ of CPO-7, ZnO, Zn_5–BPDC, and IRMOF-9, respectively, where α is the absorption coefficient. Band gaps are extrapolated from tangential lines, intersecting $(\alpha h\upsilon)^2$ at $h\upsilon = E_g$.

the band gap of Zn_5–BPDC red shifts to 3.36 eV, presumably due to the larger SBU cluster size; the band gap of CPO-7 is further shifted to 3.26 eV, which is very close to that of bulk ZnO with a value of 3.27 eV,[41] indicating the effect of the infinite layered inorganic zinc hydroxide SBUs. We should point out that IRMOF-10 would be a more direct comparison since it does not contain ligand interpenetration in the lattice structure. However, no experimental protocol has been reported in the synthesis of IRMOF-10 at present, and our experimental attempt to prepare this compound was unsuccessful. We did, however, perform DFT calculations for both systems, and the comparison between the two are given in the following discussion. A summary of the experimentally measured values in comparison with the theoretical calculations is given in Table 1.

Since the same organic linker of BPDC was used to prepare this series of MOFs, we argue that the decreasing value of the band gap with increasing cluster size could be primarily attributed to the decreasing quantum confinement effect of SBUs, which is similar to those observed for quantum dots.[28] This band-gap shift was also captured by the DFT calculations, which revealed band-gap values of 3, 2.93, and 2.76 eV for IRMOF-9, Zn_5–BPDC, and CPO-7, respectively. The results are also summarized in Table 1. Generally, the experimentally measured band-gap value is larger than the calculated results, with MOF-FMA being an exception. This is consistent with the well-documented fact that DFT usually underestimates the band gap of materials, including MOFs.[42] This issue was shown to be rectifiable in part by employing hybrid functionals, such as B3LYP.[43] However, hybrid functionals do not offer clear advantages over the pure density functionals on other properties of the MOFs. Furthermore, using hybrid functionals increases computational cost significantly for the calculations using the plane-wave-based programs such as the VASP code.

The band gap of the IRMOF-10 structure was calculated to be 3.04 eV using the VASP code and 3.10 eV using the Siesta code, demonstrating again the consistent band gap from the two different programs and highlighting the effect of interpenetration on the band gaps of MOFs. In addition, the measured energy gap for dilute BPDC ligand in solvent is 3.80 eV (Figure 3), much higher than the band gap of the

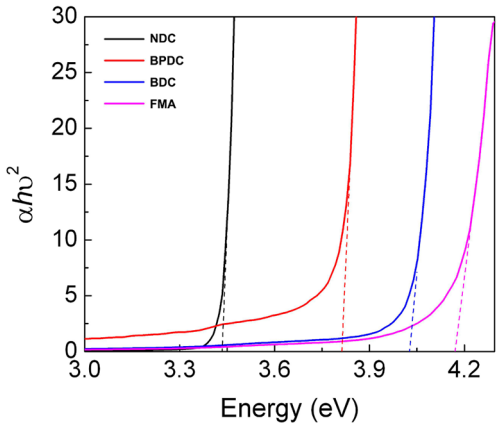

Figure 3. Electronic energy gaps of diluted (2 mM) linkers FMA, BPDC, BDC, and NDC in DMSO. Band gaps are extrapolated from the tangential line, intersecting $(\alpha h\upsilon)^2$ at $h\upsilon = E_g$, which are 4.18 eV for NDC, 4.02 eV for BDC, 3.80 eV for BPDC, and 3.38 eV for FMA.

corresponding CPO-7, Zn5-BPDC, and IRMOF-9 MOFs. This is likely due to the charge redistribution at the interface between organic linkers and inorganic SBU clusters. Such electronic interaction between organics and inorganic substrate tends to lower the interfacial energy.[44–46] This phenomenon becomes more pronounced for the larger SBUs since they provide more bonding sites with the organic linker. This is also consistent with the theoretical calculation.[26]

Table 1. Comparison of Experimental and Theoretical Band-Gap Values in MOF Systems

MOF systems	IRMOF-9	Zn5-BPDC	CPO-7	MOF-FMA	MOF-5	IRMOF-8
experiment (eV)	3.42	3.36	3.26	4.13	3.80	3.27
theory (eV)	3.00[a]	2.93	2.76	4.55[a]	3.52/3.55[a]	2.91[a]

[a]Results calculated using Siesta.

dx.doi.org/10.1021/ic301189m | Inorg. Chem. 2012, 51, 9039–9044

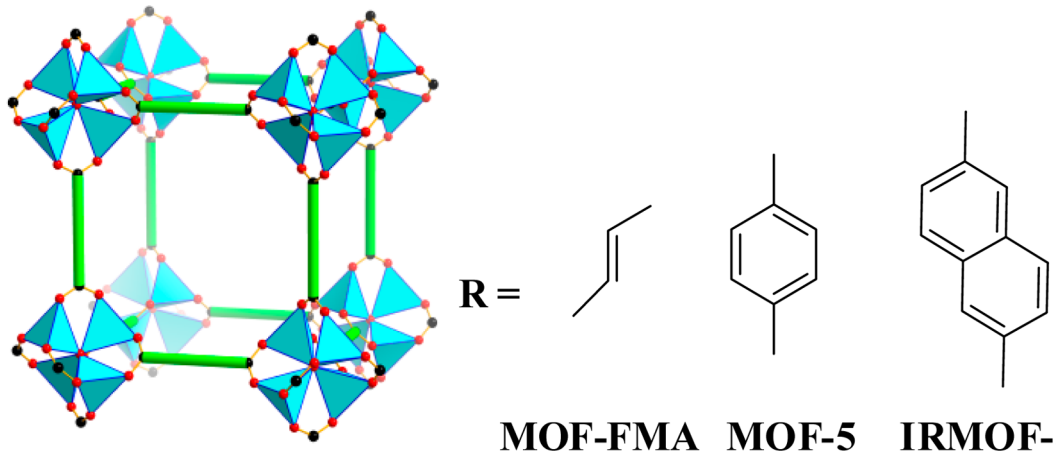

Figure 4. Structure of α-Po-typed MOFs based on Zn_4O SBU and dicarboxylate linkers with different conjugations. Color scheme: turquoise polyhedra, Zn; red sphere, O; black sphere, C; green stick, conjugated linker.

To further validate the theoretical prediction that the band gaps of MOF can be tuned by alternating the conjugation of the organic linker,[27] we chose MOF-5 (or IRMOF-1) as the prototype MOF, which is constructed by the benzene dicarboxylate (BDC) ligand and the Zn_4O cluster SBU with α-Po topology.[47] The semiconductor behavior of MOF-5 has been both experimentally and theoretically studied, which suggested that the conjugated benzene ring confers the energy transfer to the inorganic Zn_4O_{13} cluster behaving as a ZnO quantum dot.[48−52] To increase the conjugation of the dicarboxylate linker, the benzene ring was substituted with a naphthalene ring using the 2,6-naphthalene dicarboxylate (NDC) ligand, which was expected to have a narrower band gap than that of MOF-5. To decrease the conjugation of the dicarboxylate ligand, the aromatic benzene ring was replaced with a carbon−carbon double bond by employing the fumarate (FMA) ligand, which we expected to demonstrate a wider band gap compared to that of MOF-5. Under the concept of "reticular synthesis",[16−19] the connection of 2,6-naphthalene dicarboxylate with Zn_4O SBU afforded IRMOF-8,[30] while the linkage of fumarate with Zn_4O SBU led to MOF-FMA, which has the same structure as a recently reported MOF.[31] Both IRMOF-8 and MOF-FMA have the same α-Po topology as MOF-5 (Figure 4).

MOF-FMA was synthesized under solvothermal conditions by reacting $Zn(NO_3)_2{\cdot}6H_2O$ and fumaric acid in diethylformamide; MOF-5 and IRMOF-8 were prepared according to the procedures optimized by Long et al. in a recent report.[29] All three samples were activated according to the procedures in the reported literature,[31] and their identification was confirmed by the powder X-ray diffraction patterns (Figure S5, Supporting Information).

As shown in Figure 5, the measured band gap of MOF-5 is 3.80 eV, which is close to the theoretical calculation. The results are also summarized in Table 1. To explore the possible electron delocalization and energy relaxation in MOF-5 we also measured the band gap of the isolated linker BDC ligand in diluted DMSO solution and obtained a value of 4.02 eV (Figure 3). The result is also summarized in Table 2. MOF-5 possesses a red shift in band gap with respect to the isolated BDC ligand in the diluted solution. This suggests that the BDC organic linker shares electrons with Zn_4O_{13} cluster via the ligand to cluster charge transfer (LCCT), thus reducing the energy gap of the MOF, as suggested from previous experimental and

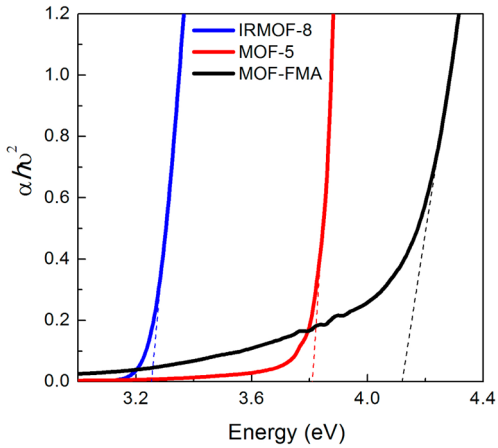

Figure 5. Band-gap energy of IRMOF-8, MOF-5, and MOF-FMA. Solid lines of blue, red, and black are the relation of $(\alpha h\upsilon)^2$ versus the photon energy $(h\upsilon)$ of IRMOF-8, MOF-5, and MOF-FMA, respectively, where α is the absorption coefficient. Band gaps are extrapolated from tangential lines, intersecting $(\alpha h\upsilon)^2$ at $h\upsilon = E_g$.

Table 2. Experimental Energy-Gap Values of Ligands

ligands	NDC	BPDC	BDC	FMA
experiment (eV)	3.38	3.8	4.02	4.18

theoretical studies.[48−53] Although the exact band gap of the Zn_4O_{13} cluster cannot be obtained, it can be inferred that its possible ZnO quantum dot behavior is overshadowed by the BDC ligand, which dominates the band gap of the whole MOF-5 framework.

To understand the impact by ligand conjugation, we then measured and calculated the band gaps of MOF-FMA and IRMOF-8, respectively. The results are also summarized in Table 1. As shown in Figure 5, MOF-FMA has a band gap of 4.13 eV while the band gap of IRMOF-8 is 3.27 eV. Given similar contributions from the carboxylate group and the Zn_4O_{13} cluster, the narrower band gap of IRMOF-8 compared to MOF-5 can be primarily attributed to the greater π conjugation in the naphthalene ring in IRMOF-8 than that in the benzene ring in MOF-5. The wider band gap observed for MOF-FMA can be mainly ascribed to the less conjugated carbon−carbon double bond compared to the benzene ring in MOF-5 or naphthalene ring in IRMOF-8. Furthermore, the

dx.doi.org/10.1021/ic301189m | Inorg. Chem. 2012, 51, 9039−9044

measured energy gaps for isolated FMA and NDC ligands in diluted solutions are 4.18 and 3.38 eV, respectively (Figure 3). The results are also summarized in Table 2. The band gaps of both MOF-FMA and IRMOF-8 exhibit red shifts in comparison to their corresponding isolated organic linkers, indicating relaxation of the interfacial energy at organic linkers and the inorganic Zn_4O_{13} clusters via interfacial charge transfer. These results support the theoretical prediction that the reduction of the conjugation of the carboxylate organic linker can widen the band gap of MOFs.

Recent photoluminescence (PL) studies indicated that the isolated ZnO impurities could affect the band gaps of MOFs.[53] To further scrutinize the purity of the MOF compounds investigated in this work, we conducted PL measurements and the spectra were normalized for comparison and are presented in Figure 6. Nanosized ZnO powders (<100 nm) exhibit the

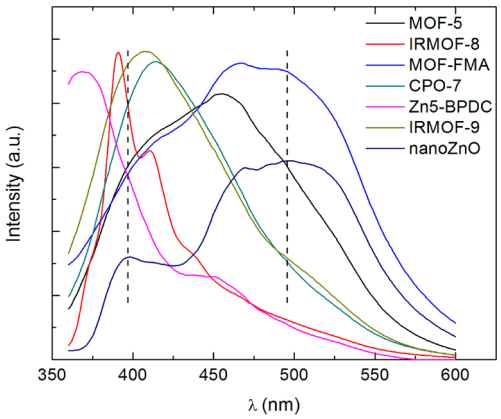

Figure 6. Photoluminescence spectra of MOF samples in comparison with bulk and nanosized ZnO.

characteristic band-gap emission around 380−390 nm and below-band-gap emission between 420 (3.0 eV) and 650 nm (1.9 eV). This emission is originated from the decay of photoexcited electrons to the surface defective trap states in ZnO, especially in nanosized ZnO as nanosized ZnO possesses more surface area, thus containing more surface defects. These defective surface states reside below the conduction band edge so that some photoexcited electrons can decay to these defective states through surface recombination, leading to long-wavelength fluorescence.[54−56] It can be seen that the PL spectra of the MOF samples do not show the characteristic band-gap emission and below-band-gap emission, indicating that the ZnO moieties in all six MOF samples are incorporated with organic linkers. Furthermore, if MOF structures collapse and yield isolated nanosized ZnO, the below-band-gap broad PL peak due to surface defects of nanosized ZnO would have been presented. These data further confirmed the purity of the prepared MOF samples, excluding the profound effects of isolated ZnO impurities on the band gaps of the investigated MOFs.

CONCLUSIONS

In summary, we demonstrated that the band-gap tunability of MOFs can be achieved via two different strategies: changing the cluster size of SBU and altering the conjugation of the organic linker. It is conceivable that an additional increase of the size of SBUs or the π conjugation of the organic ligands can further narrow MOFs' band gaps, and this aspect of work is under way in our laboratory. In perspective, it is known that many factors can also contribute to the band-gap shift in the semiconducting nanoclusters including cluster size,[57] electronic effects such as electron−phonon coupling,[58] shape effect (especially at small sizes),[59] vacancies, and other surface defects,[60,61] and so on. Therefore, the impact on the MOF's band gap by SBU could be significantly more complicated than what is discussed in this report, which serves only as the starting point. Such complexity, however, also offers more opportunities to further tune the electronic and optical properties of MOFs via new SBU design, which may find useful applications in the fields of optics and electronics.

ASSOCIATED CONTENT

Supporting Information

PXRD patterns of MOFs and structural pictures of IRMOF-9, Zn_5−BPDC, and CPO-7. This material is available free of charge via the Internet at http://pubs.acs.org.

AUTHOR INFORMATION

Corresponding Author

*E-mail: djliu@anl.gov (D.-J.L.); sqma@usf.edu (S.M.).

Notes

The authors declare no competing financial interest.

ACKNOWLEDGMENTS

This work was supported by the Office of Science, U.S. Department of Energy, under Contract DE-AC02-06CH11357. S.M. acknowledges the Director's Postdoctoral Fellowship from Argonne National Laboratory and financial support from USF. T.X. also is thankful for the support from a NIU-Argonne NanoScience Fellowship via InSET and NSF (CBET-1150617).

REFERENCES

(1) (a) Long, J. R.; Yaghi, O. M. *Chem. Soc. Rev.* **2009**, *38*, 1213−1214. (b) Zhou, H.-C.; Long, J. R.; Yaghi, O. M. *Chem. Rev.* **2012**, *112*, 673−674.

(2) (a) Ma, S. Q.; Meng, L. *Pure Appl. Chem.* **2011**, *83*, 167−188. (b) Wang, X.-S.; Meng, L.; Cheng, Q.; Kim, C.; Wojtas, L.; Chrzanowski, M.; Chen, Y.-S.; Zhang, X. P.; Ma, S. *J. Am. Chem. Soc.* **2011**, *133*, 16322−16325. (c) Wang, X.-S.; Chrzanowski, M.; Gao, W.-Y.; Wojtas, L.; Chen, Y.-S.; Zaworotko, M. J.; Ma, S. *Chem. Sci.*, **2012**, *3*, DOI: 10.1039/C2SC20330H.

(3) Murray, L. J.; Dinca, M.; Long, J. R. *Chem. Soc. Rev.* **2009**, *38*, 1294−1314.

(4) Ma, S. Q.; Zhou, H. C. *Chem. Commun.* **2010**, *46*, 44−53.

(5) Li, J. R.; Kuppler, R. J.; Zhou, H. C. *Chem. Soc. Rev.* **2009**, *38*, 1477−1504.

(6) (a) Ma, S. Q. *Pure Appl. Chem.* **2009**, *81*, 2235−2251. (b) Wang, X.-S.; Chrzanowski, M.; Kim, C.; Gao, W.-Y.; Wojtas, L.; Chen, Y.-S.; Zhang, X. P.; Ma, S. *Chem. Commun.* **2012**, *48*, 7173−7175. (c) Gao, W.-Y.; Yan, W.; Cai, R.; Meng, L.; Salas, A.; Wang, X.-S.; Wojtas, L.; Shi, X.; Ma, S. *Inorg. Chem.* **2012**, *51*, 4423−4425. (d) Gao, W.-Y.; Niu, Y.; Chen, Y.; Wojtas, L.; Cai, J.; Chen, Y.-S.; Ma, S. *CrystEngComm*, **2012**, *10*, DOI: 10.1039/c2ce25484k.

(7) Lee, J.; Farha, O. K.; Roberts, J.; Scheidt, K. A.; Nguyen, S. T.; Hupp, J. T. *Chem. Soc. Rev.* **2009**, *38*, 1450−1459.

(8) Corma, A.; Garcia, H.; Xamena, F. X. L. *Chem. Rev.* **2010**, *110*, 4606−4655.

(9) Lykourinou, V.; Chen, Y.; Wang, X. S.; Meng, L.; Hoang, T.; Ming, L. J.; Musselman, R. L.; Ma, S. *J. Am. Chem. Soc.* **2011**, *133*, 10382−10385.

(10) Chen, B. L.; Wang, L. B.; Zapata, F.; Qian, G. D.; Lobkovsky, E. B. *J. Am. Chem. Soc.* **2008**, *130*, 6718−6719.

(11) Chen, B. L.; Wang, L. B.; Xiao, Y. Q.; Fronczek, F. R.; Xue, M.; Cui, Y. J.; Qian, G. D. *Angew. Chem., Int. Ed.* **2009**, *48*, 500−503.
(12) Chen, B. L.; Xiang, S. C.; Qian, G. D. *Acc. Chem. Res.* **2010**, *43*, 1115−1124.
(13) Taylor, K. M. L.; Rieter, W. J.; Lin, W. B. *J. Am. Chem. Soc.* **2008**, *130*, 14358−14359.
(14) An, J. Y.; Geib, S. J.; Rosi, N. L. *J. Am. Chem. Soc.* **2009**, *131*, 8376−8377.
(15) Horcajada, P.; Chalati, T.; Serre, C.; Gillet, B.; Sebrie, C.; Baati, T.; Eubank, J. F.; Heurtaux, D.; Clayette, P.; Kreuz, C.; Chang, J. S.; Hwang, Y. K.; Marsaud, V.; Bories, P. N.; Cynober, L.; Gil, S.; Ferey, G.; Couvreur, P.; Gref, R. *Nat. Mater.* **2010**, *9*, 172−178.
(16) Eddaoudi, M.; Moler, D. B.; Li, H. L.; Chen, B. L.; Reineke, T. M.; O'Keeffe, M.; Yaghi, O. M. *Acc. Chem. Res.* **2001**, *34*, 319−330.
(17) Yaghi, O. M.; O'Keeffe, M.; Ockwig, N. W.; Chae, H. K.; Eddaoudi, M.; Kim, J. *Nature* **2003**, *423*, 705−714.
(18) Ockwig, N. W.; Delgado-Friedrichs, O.; O'Keeffe, M.; Yaghi, O. M. *Acc. Chem. Res.* **2005**, *38*, 176−182.
(19) Tranchemontagne, D. J.; Mendoza-Cortes, J. L.; O'Keeffe, M.; Yaghi, O. M. *Chem. Soc. Rev.* **2009**, *38*, 1257−1283.
(20) Perry, J. J.; Perman, J. A.; Zaworotko, M. J. *Chem. Soc. Rev.* **2009**, *38*, 1400−1417.
(21) Allendorf, M. D.; Bauer, C. A.; Bhakta, R. K.; Houk, R. J. T. *Chem. Soc. Rev.* **2009**, *38*, 1330−1352.
(22) Silva, C. G.; Corma, A.; Garcia, H. *J. Mater. Chem.* **2010**, *20*, 3141−3156.
(23) Fang, Q. R.; Zhu, G. S.; Jin, Z.; Xue, M.; Wei, X.; Wang, D. J.; Qiu, S. L. *Angew. Chem., Int. Ed.* **2006**, *45*, 6126−6130.
(24) Fang, Q. R.; Zhu, G. S.; Xue, M.; Zhang, Q. L.; Sun, J. Y.; Guo, X. D.; Qiu, S. L.; Xu, S. T.; Wang, P.; Wang, D. J.; Wei, Y. *Chem.—Eur. J.* **2006**, *12*, 3754−3758.
(25) Dan-Hardi, M.; Serre, C.; Frot, T.; Rozes, L.; Maurin, G.; Sanchez, C.; Ferey, G. *J. Am. Chem. Soc.* **2009**, *131*, 10857−10859.
(26) Kuc, A.; Enyashin, A.; Seifert, G. *J. Phys. Chem. B* **2007**, *111*, 8179−8186.
(27) Gascon, J.; Hernandez-Alonso, M. D.; Almeida, A. R.; van Klink, G. P. M.; Kapteijn, F.; Mul, G. *ChemSusChem* **2008**, *1*, 981−983.
(28) Peng, X. G. *Acc. Chem. Res.* **2010**, *43*, 1387−1395.
(29) Kaye, S. S.; Dailly, A.; Yaghi, O. M.; Long, J. R. *J. Am. Chem. Soc.* **2007**, *129*, 14176−14177.
(30) Eddaoudi, M.; Kim, J.; Rosi, N.; Vodak, D.; Wachter, J.; O'Keeffe, M.; Yaghi, O. M. *Science* **2002**, *295*, 469−472.
(31) Xue, M.; Liu, Y.; Schaffino, R. M.; Xiang, S. C.; Zhao, X. J.; Zhu, G. S.; Qiu, S. L.; Chen, B. L. *Inorg. Chem.* **2009**, *48*, 4649−4651.
(32) Fang, Q. R.; Zhu, G. S.; Jin, Z.; Xue, M.; Wei, X.; Wang, D. J.; Qiu, S. L. *Cryst. Growth Des.* **2007**, *7*, 1035−1037.
(33) Kongshaug, K. O.; Fjellvag, H. *J. Solid State Chem.* **2004**, *177*, 1852−1857.
(34) Kubelka, P.; Munk, F. *Z. Tech. Phys.* **1931**, *12*, 593−601.
(35) Kresse, G.; Hafner, J. *Phys. Rev. B* **1993**, *48*, 13115−13118.
(36) Kresse, G.; Furthmuller, J. *Comput. Mater. Sci.* **1996**, *6*, 15−50.
(37) Blochl, P. E. *Phys. Rev. B* **1994**, *50*, 17953−17979.
(38) Kresse, G.; Joubert, D. *Phys. Rev. B* **1999**, *59*, 1758−1775.
(39) Perdew, J. P.; Burke, K.; Ernzerhof, M. *Phys. Rev. Lett.* **1996**, *77*, 3865−3868.
(40) Soler, J. M.; Artacho, E.; Gale, J. D.; García, A.; Junquera, J.; Ordejón, P.; Sánchez-Portal, D. *J. Phys.: Condens. Matter* **2002**, *14*, 2745−2779.
(41) Law, M.; Greene, L. E.; Johnson, J. C.; Saykally, R.; Yang, P. D. *Nat. Mater.* **2005**, *4*, 455−459.
(42) Yang, L. M.; Vajeeston, P.; Ravindran, P.; Fjellvag, H.; Tilset, M. *Inorg. Chem.* **2010**, *49*, 10283−10290.
(43) Civalleri, B.; Napoli, F.; Noel, Y.; Roetti, C.; Dovesi, R. *CrystEngComm* **2006**, *8*, 364−371.
(44) Braun, S.; Salaneck, W. R.; Fahlman, M. *Adv. Mater.* **2009**, *21*, 1450−1472.
(45) Sessolo, M.; Bolink, H. J. *Adv. Mater.* **2011**, *23*, 1829−1845.
(46) Ishii, H.; Sugiyama, K.; Ito, E.; Seki, K. *Adv. Mater.* **1999**, *11*, 605−625.
(47) Li, H. L.; Eddaoudi, M.; O'Keeffe, M.; Yaghi, O. M. *Nature* **1999**, *402*, 276−279.
(48) Bordiga, S.; Lamberti, C.; Ricchiardi, G.; Regli, L.; Bonino, F.; Damin, A.; Lillerud, K. P.; Bjorgen, M.; Zecchina, A. *Chem. Commun.* **2004**, 2300−2301.
(49) Alvaro, M.; Carbonell, E.; Ferrer, B.; Xamena, F. X. L. I.; Garcia, H. *Chem.—Eur. J.* **2007**, *13*, 5106−5112.
(50) Xamena, F. X. L. I.; Corma, A.; Garcia, H. *J. Phys. Chem. C* **2007**, *111*, 80−85.
(51) Tachikawa, T.; Choi, J. R.; Fujitsuka, M.; Majima, T. *J. Phys. Chem. C* **2008**, *112*, 14090−14101.
(52) Choi, J. H.; Choi, Y. J.; Lee, J. W.; Shin, W. H.; Kang, J. K. *Phys. Chem. Chem. Phys.* **2009**, *11*, 628−631.
(53) Feng, P. L.; Perry, J. J.; Nikodemski, S.; Jacobs, B. W.; Meek, S. T.; Allendorf, M. D. *J. Am. Chem. Soc.* **2010**, *132*, 15487−15489.
(54) Fonoberov, V. A.; Balandin, A. A. *Appl. Phys. Lett.* **2004**, *85*, 5971−5973.
(55) Kenanakis, G.; Androulidaki, M.; Koudoumas, E.; Savvakis, C.; Katsarakis, N. *Superlattices Microstruct.* **2007**, *42*, 473−478.
(56) Shalish, I.; Temkin, H.; Narayanamurti, V. *Phys. Rev. B* **2004**, *69*, 245401.
(57) Yang, Q.; Tang, K.; Zuo, J.; Qian, Y. *Appl. Phys. A: Mater. Sci. Process.* **2004**, *79*, 1847−1851.
(58) Ray, S. C.; Low, Y.; Tsai, H. M.; Pao, C. W.; Chiou, J. W.; Yang, S. C.; Chien, F. Z.; Pong, W. F.; Tsai, M. H.; Lin, K. F.; Cheng, H. M.; Hsieh, W. F.; Lee, J. F. *Appl. Phys. Lett.* **2007**, *91*, 262101−3.
(59) Yang, P.; Yan, H.; Mao, S.; Russo, R.; Johnson, J.; Saykally, R.; Morris, N.; Pham, J.; He, R.; Choi, H. J. *Adv. Funct. Mater.* **2002**, *12*, 323−331.
(60) Djurišić, A. B.; Leung, Y. H. *Small* **2006**, *2*, 944−961.
(61) Yang, Y.; Yan, X. H.; Xiao, Y.; Lu, D. *Appl. Phys. Lett.* **2010**, *97*, 033106−3.